Geophysical Research Letters

RESEARCH LETTER
10.1029/2020GL090364

Converging Luminosity in Column-Sprite Filaments

Z. Gomez Kuri[1], S. Soula[1], T. Neubert[2], J. Mlynarczyk[3], and C. Köhn[2]

[1]Laboratoire d'Aérologie, Université de Toulouse III, CNRS, Toulouse, France, [2]National Space Institute, Technical University of Denmark, Lyngby, Denmark, [3]Department of Electronics, AGH University of Science and Technology, Krakow, Poland

Key Points:

- A sprite event presented 8 simultaneous columns with converging luminosity in their filaments
- Cloud-top temperature, lighting and magnetic field data are used to study the atmospheric conditions
- Detachment of electrons from negative ions may drive the long-lasting currents in the sprite filaments

Supporting Information:

- Supporting Information S1
- Movie S1

Correspondence to:
Z. Gomez Kuri,
zgomez.kuri@gmail.com

Citation:
Gomez Kuri, Z., Soula, S., Neubert, T., Mlynarczyk, J., & Köhn, C. (2021). Converging luminosity in column-sprite filaments. *Geophysical Research Letters*, *48*, e2020GL090364. https://doi.org/10.1029/2020GL090364

Received 21 AUG 2020
Accepted 16 FEB 2021

Abstract Sprites are electrical discharges in the mesosphere powered by the quasi-electrostatic field following a cloud-to-ground lightning stroke. They are luminous structures with tendrils formed by a space charge wave with high electric fields that ionizes the atmosphere, excites optical emissions and leaves a trail of enhanced densities of electrons, and negative and positive ions. The duration of the luminous streamers in sprites is usually ~1–10 ms. In this study, we present observations of sprite streamer filaments where the upper and lower ends continue to glow for more than 80 ms while the two ends slowly converge and fade. Simultaneous magnetic observations suggest that the field in the mesosphere is maintained at a high value by the long-lasting continuing current of the causative stroke. We propose that the observation is a signature of currents in the filaments fed by electrons detached from negative ions at the lower origin.

Plain Language Summary Sprites are electrical discharges above thunderstorms that occur after a cloud-to-ground lightning stroke. Most commonly observed by video cameras at standard frame rates, they appear as luminous structures with tendrils that can extend from 85 to 50 km in altitude. They can be shaped like carrots, jellyfish or columns, the latter of which usually propagate downwards. The filaments in sprites are actually streamers that remain luminous for ~1–10 ms and propagate with velocities in the order of 10^7 m s^{-1}. In this study, we present video camera observations of streamer filaments in column sprites where the upper and lower ends continue to glow for more than 80 ms while the two ends slowly converge and fade. Simultaneous magnetic observations suggest that the electric field at the altitude of the observations is maintained at a high value by a long-lasting continuing current of the causative stroke. We propose that the observation is a signature of currents in the filaments fed by electrons detached from negative ions at the lower origin.

1. Introduction

Sprites are optical flashes above thunderclouds that occur at altitudes between 50 and 85 km (Sentman et al., 1995). They are discharges powered by the quasi-electrostatic field in the mesosphere produced by the sudden charge removal from a cloud by a cloud-to-ground (CG) lightning stroke (Pasko et al., 1997), usually of positive polarity (Williams et al., 2007). Sprites are most commonly observed with video cameras at ~25 frames per second and are often seen in one or two frames only, where they appear as luminous filaments that may range in numbers from a single to a bundle of filaments with a complex structure (Pasko et al., 2012). These filaments are streamers: wave packets of enhanced space charge and electric field that adds to the ambient field in front of the wave and reduces the field behind it. The enhanced field at the wavefront allows streamers to propagate into regions where the background field is below the threshold for discharge. The threshold field, E_k, is the field at which the source of free electrons, created by electron impact ionization of the neutral atmosphere, equals the loss of electrons by attachment to neutrals. It is approximately proportional to the neutral density, n_n, and is often expressed as the *reduced* field E_k/n_n (Raizer, 1997). At sea level E_k ~3.2 MV m^{-1}, $n_n \approx 2.8 \times 10^{25}$ m^{-3}, and at 70 km E_k ~190 V m^{-1}, $n_n \approx 1.7 \times 10^{21}$ m^{-3}. The neutral density is also important for the time scales of discharges, which is approximately proportional to $1/n_n$ (Ebert et al., 2010) and therefore varies by 1 to 2 orders of magnitude along a streamer channel. The duration of the luminous streamers is usually ~1–10 ms and is determined by the time scale of the quasi-electrostatic field in the mesosphere or the transit time of the luminous wavefront. Incepted at high altitudes by the sudden onset of a high electric field in the region, the space charge waves plow downwards

through the atmosphere at ~10^7 m/s, leaving in their wake a trail of free electrons, and negative and positive ions.

The structure and dynamics of sprites can have various degrees of complexity depending on the number of filaments generated. Although not completely understood, it appears that the electromagnetic fields radiated by lightning currents may play a role in the formation of their luminous patterns (Asano et al., 2009; Cho & Rycroft, 2001; van der Velde et al., 2006), as well as small-scale inhomogeneities of the mesosphere (Köhn et al., 2019; Qin et al., 2014; Suszcynsky et al., 1999). Imaging at several thousand frames per second shows that the filament channels are not luminous during their whole length, but rather at the streamer wavefront, with growing emission intensities at the upper end, sometimes with localized luminous beads in the filament channel, and emission of secondary streamers (Montanyà et al., 2010; Stenbaek-Nielsen et al., 2013). These glows and beads can propagate within the ionized channel formed by the streamers at velocities of 10^4 m s^{-1} (Gerken & Inan, 2002) or be stationary (Cummer et al., 2006; Luque et al., 2016; Malagón-Romero et al., 2020; Stenbaek-Nielsen et al., 2013).

In rare cases, converging motion of the luminosity within an ionized channel can occur such as the observation presented in Figure 11 of Stenbaek-Nielsen and McHarg (2008). Here, we present observations of streamer filaments of a sprite that exhibits converging upward and downward luminosity in 8 columns. The long duration of the luminous event, ~160 ms, brings not only electron ionization and attachment into play, the most commonly discussed processes of streamer dynamics, but also electron detachment, which operates at lower field intensities and longer time scales. We first present the observation of the eight simultaneous converging sprites and the overall storm context of these, and then offer a discussion.

2. Data Acquisition

The optical observations were made with a video camera from Observatoire Midi Pyrénées on the summit of Pic du Midi at 2,877 m altitude. The camera used was a low-light Watec 902H model with 1/2″ Sony ICX-429ALL ExView CCDs with a sensitivity rated at 0.0001 lux. The lens was F1.4 with a 31° horizontal field-of-view. The software *Cartes du Ciel* was used to obtain the azimuth and elevation of the observed events by comparing the background stars in the images, and the altitude of the sprite elements was estimated using the location of the causative lightning stroke as the distance to the events. The velocity of each sprite element was calculated using their change in altitude in successive de-interlaced fields recorded 20 ms apart.

The data on lightning activity is from the Lightning Network (LINET), which detects radio waves from lightning sources in the VLF/LF band (3–300 kHz). The network determines the 3D position of the sources, which allows for detection of both intra-cloud (IC) and CG lightning, and gives the peak current, time and location of each stroke as well as the altitude of the IC strokes (Betz et al., 2009). ELF measurements in the frequency range 0.03–300 Hz from the Hylaty Geophysical Station (Kulak et al., 2014) were used to determine the current moment and charge moment change (CMC) of the sprite associated lightning discharge, which suggest the presence of a long-duration electric field in the mesosphere. The current moment change was calculated using the method presented by Mlynarczyk et al. (2015). The overall storm properties are characterized by cloud top temperature data measured by the SEVIRI instrument (Spinning Enhanced Visible and Infrared Imager) on the Meteosat Second Generation satellite.

3. Observations and Analysis

On July 5th, 2017, we observed 13 sprite events over the trailing stratiform region of a mesoscale convective system passing through northern Spain. One event consisted of eight column sprites generated by the same lightning stroke. It is shown in Figure 1a. Each element consists of two luminous regions; a longer one at higher altitudes and a shorter region at lower altitudes. The two regions converge in time, as seen in the consecutive images discussed below. The cloud-top temperature is shown in Figure 1b and zoomed to the region of the lightning activity in Figure 1c. The lowest cloud-top temperature of the system was ~−60°C at 19:55 and 20:55 UTC, typical for the convective region of thunderstorms in Europe (Savtchenko et al., 2009; Soula et al., 2009). The sprite columns are numbered from 1 to 8, counting from left to right in the image in

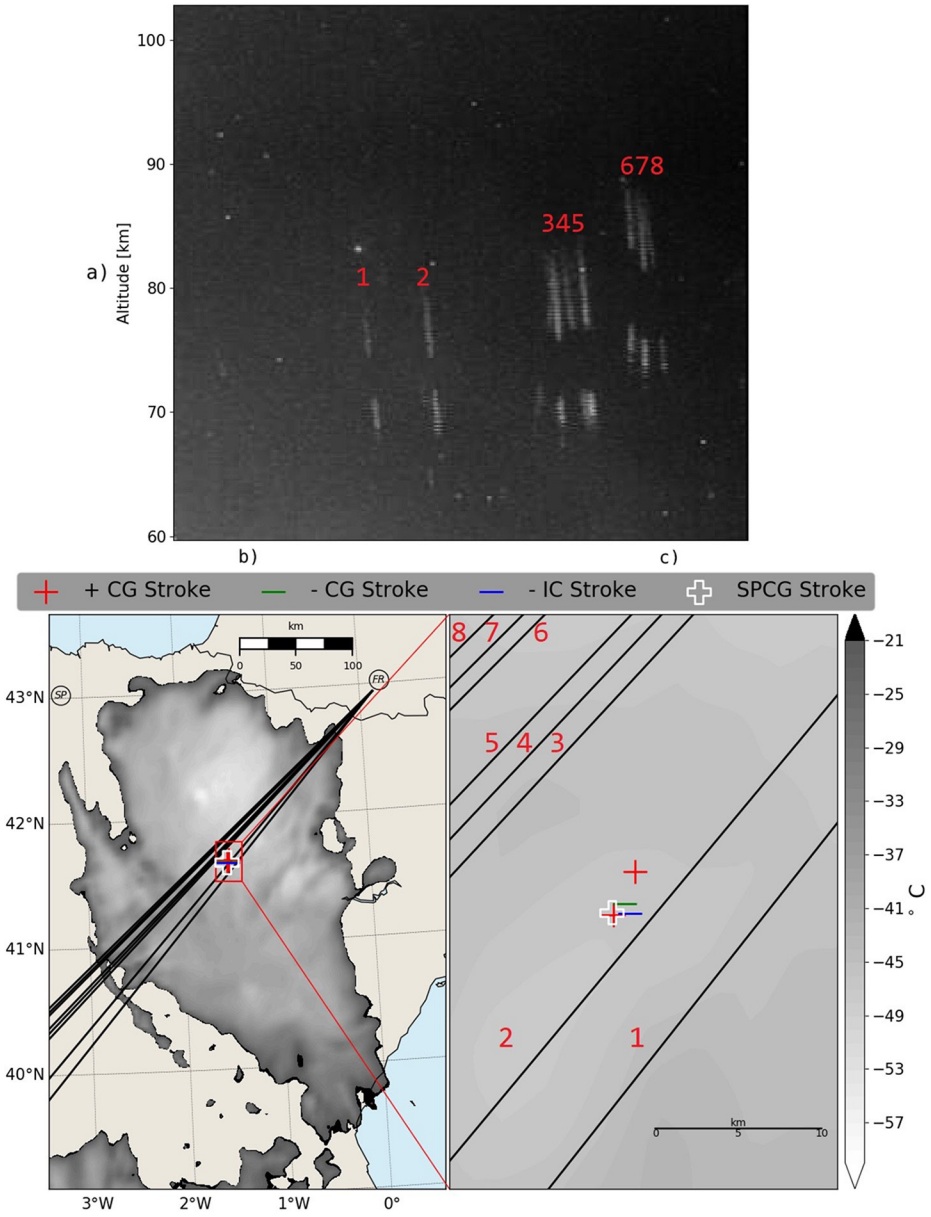

Figure 1. (a) Observation of eight column sprites with converging luminosity from Pic du Midi. The image is the cumulative luminosity obtained by combining all of the frames in the 1.04 s video starting at 22:39:30.663 UTC on 2017-07-05. (b) The cloud-top temperature map at 22:40 UTC with the line-of-sight of each column and (c) zoomed to the region of the sprite producing CG (SPCG) stroke (highlighted with the white cross) and related lightning activity.

Figure 1a. The sprite producing CG (SPCG) stroke is marked with a white cross and the related activity by red, green, and blue markers depending on the type of stroke.

The main stroke had a peak current of 69 kA and the related lightning strokes had peak currents less than ±5 kA. The search criteria for finding the flash producing the sprite event was defined as the group of strokes occurring within 10 km and 1 s of each other. This resulted in 4 strokes that occurred within a time window of 300 ms and within ~4 km from the line-of-sight of the second column sprite. The horizontal ground distance between each column sprite was calculated by keeping a constant latitude at the location of the parent CG stroke and calculating the ground distance between the lines of sight of each column. The distances between the columns are ~6 km for 1 and 2, ~3 km for columns 3–5, and ~1 km for 6–8. Columns 6–8 are probably ~18 km closer to the observer as they appear at a higher altitude in the image in Figure 1a.

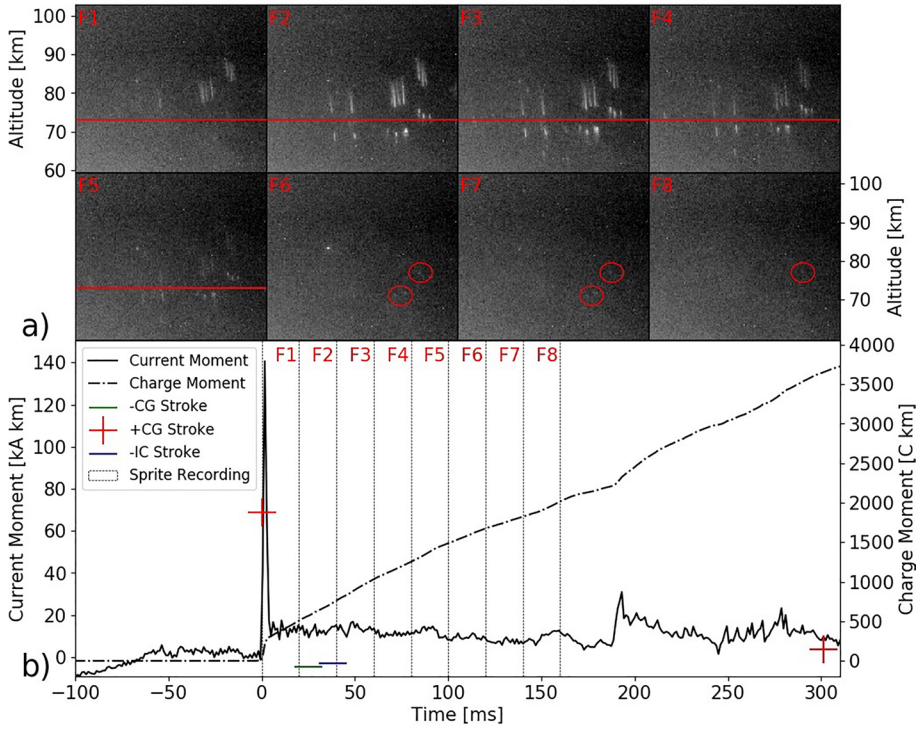

Figure 2. Sprite activity and charge and current moments of the causative stroke. (a) Images of the event with a gray scale in arbitrary units. The altitude scale is approximate and only applies for columns 1–5 (counting from the left). The red line indicates an altitude of 73 km and the red circles identify elements that are still visible until the 8th field. (b) The charge- and current moment waveforms. Time is from the causative CG stroke at 22:39:31.064 UTC. The + and − CG strokes from Figure 1c are also plotted with their peak current in kA corresponding to the left axis.

This distance is an approximation assuming that these columns also initiated at ~80 km and using the ground distance from the camera to the SPCG.

The full video is provided in the supporting information, however the sequence is shown in Figure 2a. The images shown are the de-interlaced fields, each representing 20 ms (the interlaced fields have 40 ms exposure), showing the full ~160 ms duration of the event. The sprite event started with the causative stroke at 22:39:31.064 UTC and the 8 column sprites are first seen in the field beginning at 22:39:31.063 UTC. Although the field starts 1 ms before the stroke, the sprite is likely observed after it as the de-interlaced fields show the luminosity integrated over 20 ms. The full length of the columns, including the upper and lower luminous regions, appears in the second field and continues to glow in this configuration during the following fields. In field 6 most columns disappear except the lower regions of columns 4–6, which persist until field 7 (highlighted by red circles) the latter of which lasts until field 8. The red horizontal line is an altitude reference that helps to show how the upper and lower luminous regions appear to approach each other in time, the lower element moving upwards and the upper one moving downwards. The average vertical velocity of the approaching elements was estimated as $\sim 3 \times 10^4$ m s^{-1}.

The charge and current moments of the causative flash are shown in Figure 2b. The peak currents of the strokes, including the SPCG, are also plotted and correspond to the left axis. There were also two negative CG and IC strokes during the second field of the sequence, with smaller peak currents of −4.6, and −2.9 kA, respectively and a positive CG stroke 301 ms after the SPCG also of a small peak current (3.6 kA); their contributions are ignored. The CMC during the event is substantial with a value of 3,769 C km due to the continuing current which ends 320 ms after the return stroke. The CMC continues to increase during the event, suggesting that a high electric field is maintained in the mesosphere as predicted by models (Gamerota et al., 2011).

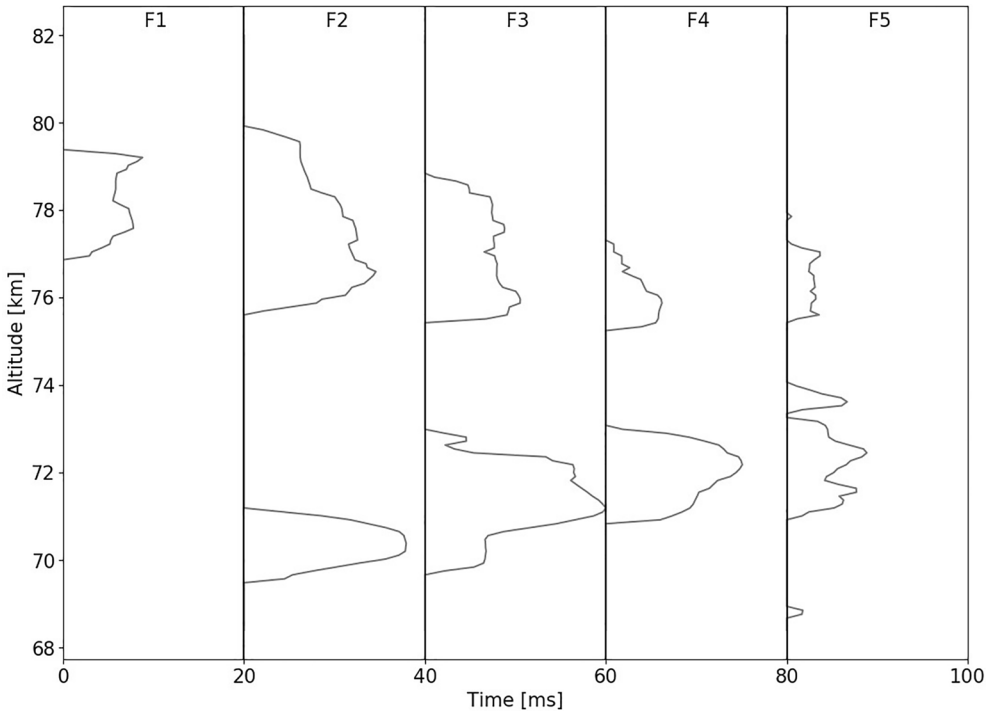

Figure 3. Altitude of the luminous regions of column sprite two in the first 5 consecutive fields of the event. The curves show the sum of the pixel values above the noise level within a camera pixel row. Each row is translated into an estimated altitude. Time is measured from the start of the exposure of the first field of the sequence: 22:39:31.063 UTC. The amplitudes of the integrated luminosities are on an arbitrary scale, but unchanged between fields.

We have quantified the motion of the luminous regions by analyzing column sprite 2. The columns are almost vertical, making it simple to estimate a unique altitude to each row of the camera CCD (the camera is mounted horizontally). The integrated luminosity of the column has been determined for each row (altitude) by summing the values above the noise level of pixels in the column and is shown in Figure 3a. This figure illustrates that the luminous regions converge, the lower region moving upwards as fast as 1.1×10^5 m s^{-1} and the upper region moving downwards at a maximum velocity of 0.8×10^5 m s^{-1}. The convergence of the regions is discussed in the next section.

4. Discussion

The column sprites that we analyze here have perhaps the simplest structure seen in sprites. The luminous regions are caused by electron impact excitation of the neutral constituents of the atmosphere. Reaching observable emission rates requires high electric fields to accelerate electrons to sufficient energies. The luminous regions of sprite streamers are therefore usually in the streamer heads, where the space charge electric field is large. In the observations we report here, we first see a rapid formation of the column sprites to their full altitudinal extent. The streamer tip velocity during this stage is not resolved with our camera's low frame rate and sensitivity, but it is likely of the order of 10^7 ms^{-1}, as reported by others (Stenbaek-Nielsen et al., 2013). The ambient quasi-electrostatic field from the positive, causative lightning discharge is pointing downwards, and the streamer is then a positive streamer with positive excess space charge in the tip. As the wave propagates downwards through the atmosphere, the constituents are ionized, leaving behind a trail of free electrons and positive ions. The ions can be considered as stationary on the time scales reported here, thus the currents are carried by the drift of electrons. The currents are driven by an electric field in the channels that is small relative to the ambient field because of the higher conductivity inside the channels. The current amplifies, or maintains, the positive space charge at the tip of a streamer, assisting its propagation (Raizer, 1997).

The background electric field is maintained by the CMC caused by the lightning continuing current in the cloud below, as predicted by models (Li et al., 2008). The duration of the CMC, and the glow of the lower tip and the upper segment of the streamer filament, is several tens of milliseconds, suggesting that the current in the filaments continues to transport electrons upwards in the filaments, thereby maintaining regions of positive space charge at the lower end and a negative space charge in the upper end. It further appears that the two space charge regions are associated with high electric fields that make both ends of the filaments glow. The above scenario is according to the model proposed by Luque and Ebert (2010). Since we do not observe secondary streamers at either end of the filaments, secondary streamer activity is likely modest and the magnitude of the total field in the glowing regions (the space charge and the ambient field) is likely of the order of E_k. The limit on the ambient field for positive streamer propagation (after they have been formed) is ~1/7 E_k and ~1/2.5 E_k for negative streamers (Pasko et al., 2000), which then are the likely maximum of the background field of the mesosphere at the lower and upper regions.

We next discuss why the glowing regions at the upper and lower ends of a filament appear to converge with time. The main processes that affect the density of electrons are ionization, attachment to N_2 and O_2, and associative detachment from negative ions (Gordillo-Vázquez & Luque, 2010) such as:

$$O^- + N_2 \Rightarrow N_2O + e^-$$

The reaction rates increase with the amplitude of the electric field. Detachment dominates at lowest amplitudes but the reaction rate is small and is not important for sprites that last less than ~10 ms (Neubert & Chanrion, 2013). Ionization dominates at the highest amplitudes and the threshold field for discharges is usually defined as the value where attachment balances ionization, that is, where the source and loss of electrons are equal (Raizer, 1997). The rapid establishment of the sprite filaments to their full extent can then be understood in terms of ionization and attachment alone, whereas the dynamics on a scale of several tens of milliseconds, when the luminous regions converge, suggest we also consider the effects of detachment.

We can get some insights from the analytical formulation of Neubert and Chanrion (2013), where the rate of change with time t in the electron and negative ion densities, $n_{e,i}$ is:

$$\begin{aligned} \frac{\partial n_e(t)}{\partial t} &= (\gamma_i - \gamma_a) n_e(t) + \gamma_d n_i(t) \\ \frac{\partial n_i(t)}{\partial t} &= \gamma_a n_e(t) - \gamma_d n_i(t) \end{aligned} \tag{1}$$

The ionization, attachment, and detachment rates, $\gamma_{i,a,d}$, depend on the electric field. In the simple formulation above, we have no electron charge transport from currents. Furthermore, the parameters include the neutral density and, for simplification, we do not distinguish between O_2 and N_2 densities, as these are included in the rates with the assumption that $n_{N_2} = 4n_{O_2}$. The formulation is similar to the one of Luque and Ebert (2010), except for the addition of the detachment term. This term makes the problem more complex because it involves n_i and then requires two equations.

The solutions to the electron and ion densities are a combination of two exponential functions with time constants τ_1 and $-\tau_2$ with $\tau_1, \tau_2 > 0$. In the asymptotic limit where $t \gg \tau_2$ only function 1 contributes, which corresponds to densities increasing with time. In this limit, one finds:

$$\frac{n_i(t)}{n_e(t)} = \eta_a(E) > 0 \tag{2}$$

The parameter η_a is a combination of reaction rates (a stands here for "asymptotic") (Neubert & Chanrion, 2013). Equation 2 implies that, barring charge transport from currents, the densities grow for all values of the electric field. Inserting Equation 2 into Equation 1 we get:

$$\frac{\partial n_e(t)}{\partial t} = (\gamma_i - \gamma_a + \gamma_d \eta_a) n_e(t) \tag{3}$$

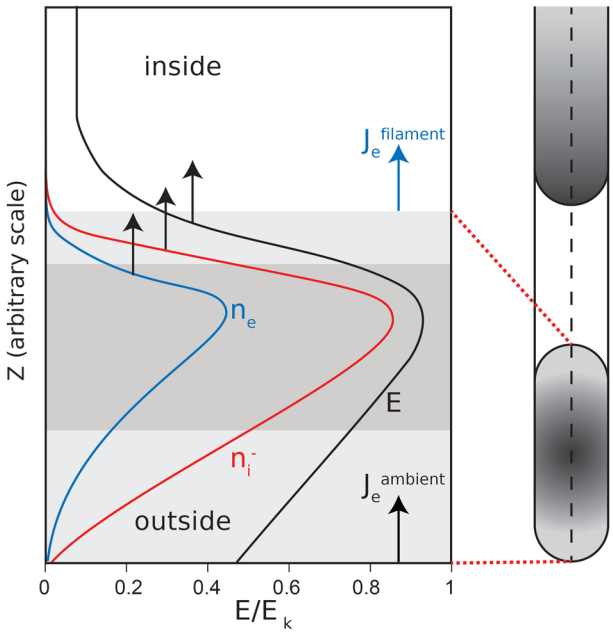

Figure 4. A snapshot in time of the electric field in the lower positive glowing region of the streamer filament at its maximum extent. The field is on the axis of symmetry (dashed line in the sketch on the right), pointing downwards. The negative ion and electron densities that develop from Equation 1 are shown (arbitrary scale). The shaded region is dominated by attachment and it corresponds to the lower luminous region as shown with the red dashed lines. The darkest region is where $E/E_k > 0.75$ corresponding to the dashed line in the plot. The arrows under $J_e^{ambient}$ and $J_e^{filament}$ are in the direction of the electron drift velocities (see text). The arrows on the curves indicate the direction of their displacement during the migration of the luminous regions.

which defines the time constant as $\tau_1 = \gamma_i - \gamma_a + \gamma_d\eta_a > 0$. The time scale τ_2 determines how fast we approach the asymptotic limit. It is 0.1–1 ms for $\frac{E}{E_k} < 1$ in the altitude range considered here, which brings us into the asymptotic regime after ~1–10 ms, i.e. within the first field. After this time, the electron and negative ion densities continue to grow, even in regions where $\frac{E}{E_k} < 1$; however, the growth rate decreases rapidly with decreasing field amplitude. The time scale that is relevant for the dynamics we study here is several tens of milliseconds, suggesting that the time constant of growth τ_1 should be < 10 ms to be relevant. We find that at altitudes around 75 km we must have $\frac{E}{E_k} > 0.75$ (Neubert & Chanrion, 2013, Figure 4). As $\tau_1 \propto 1/n_n$ the growth rate is faster at the lower end of the streamers than at the upper end by an order of magnitude or more.

In the formulation outlined above, the electric field is imposed from the outside and is unaffected by ionization, attachment and detachment, because without currents and gradients, the space charge density remains constant. This is not the case in the problem we want to study, where we expect there are gradients and currents in the luminous regions. However, since these are maintained for tens of milliseconds, we suggest that the high electric fields of the regions are maintained and that the electric field structure is almost constant. From the above analysis, we then conclude that in regions of a luminous structure, where $E/E_k > 0.75$, we may have a reservoir of free electrons.

A conceptual model of the processes in the lower positive luminous region, based on Equations 1–3, is outlined in Figure 4. The figure shows the normalized electric field magnitude, $\frac{E}{E_k}$, on the axis of symmetry of a filament between the red lines. The electron current from the ambient atmosphere flowing into the region is $J_e^{ambient}$, the electron current flowing from the region into the filament channel is $J_e^{filament}$. The sign of the current is in the direction of the electron drift. The negative ion density arising from attachment is n_i and the density of free electrons is n_e. We do not follow the positive ion densities which form a background of positive space charge. Detachment, attachment and ionization occurs throughout the region. In the unshaded region, detachment dominates, but with a small rate, and in the shaded regions, attachment dominates. Exponential growth of n_e, n_i, occurs throughout the region, but is only of a magnitude relevant to our problem in the dark shaded region where $\frac{E}{E_k} > 0.75$, which forms a source of free electrons feeding $J_e^{filament}$. The overall polarity of the region is positive (positive ion densities are not shown). The region is observed to migrate upwards, which limits the time that a volume of the atmosphere is exposed to the high fields, and thereby limits the growth of n_e, n_i in that volume.

We suggest that the electron current from the ambient atmosphere ($J_e^{ambient}$) tends to dissipate the overall positive space charge of the lower tip, while the electron current from the tip upwards in the filament channel ($J_e^{filament}$), driven by the continued background electric field, tends to enhance the overall space charge. As the tip continues to glow, the electric field and the overall positive space charge in the tip are maintained, from which follows that $J_e^{ambient} \sim J_e^{filament}$. We suggest that the luminous region migrates upward because the neutralizing negative space charge of the ambient electron current tends to accumulate at its lowest edge (outside), whereas the electron current upward in the filament channel tends to increase the positive space charge at its upper edge (inside). Without the continued background electric field powering

$J_e^{filament}$, $J_e^{ambient}$ would neutralize the positive space charge, the space charge field would decrease and the glow would extinguish, as commonly observed in sprites. A similar process occurs in the upper luminous region resulting in the two regions migrating toward each other, reducing the length of the filament channel.

5. Summary

The observed sprite event displayed eight simultaneous columns that showed converging luminosity in individual streamer channels lasting up to 160 ms. This observation suggests that detachment of electrons becomes important, driving long-lasting currents in streamer filaments, when there is a continuous current in the parent CG stroke. The current in the streamer filament drives the space charge upward in the positive (lower) tip and feeds the space charge in the negative (upper) tip of the streamer channel explaining the converging motion of the luminosity. The analytical formulation presented here can be used for modeling the phenomenon in future work.

Data Availability Statement

The video is provided in the supplementary material and all other data are available at https://doi.org/10.5281/zenodo.3994236.

Acknowledgments
This project has received funding from the European Union's Horizon 2020 Research and Innovation Program under the Marie Sklodowska-Curie grant agreement 722337. The authors thank the French consortium ICARE for the cloud-top temperature issued from Meteosat satellite and the LINET network in Spain for providing the lightning data.

References

Asano, T., Suzuki, T., Hiraki, Y., Mareev, E., Cho, M. G., & Hayakawa, M. (2009). Computer simulations on sprite initiation for realistic lightning models with higher-frequency surges. *Journal of Geophysical Research*, *114*, A02310. https://doi.org/10.1029/2008JA013651

Betz, H. D., Schmidt, K., Laroche, P., Blanchet, P., Oettinger, W. P., Defer, E., et al. (2009). LINET - An international lightning detection network in Europe. *Journal of Atmospheric Research*, *91*, 564–573. https://doi.org/10.1016/j.atmosres.2008.06.012

Cho, M., & Rycroft, M. J. (2001). Non-uniform ionisation of the upper atmosphere due to the electromagnetic pulse from a horizontal lightning discharge. *Journal of Atmospheric and Solar-Terrestrial Physics*, *63*, 559–580.

Cummer, S. A., Jaugey, N., Li, J., Lyons, W. A., Nelson, T. E., & Gerken, E. A. (2006). Submillisecond imaging of sprite development and structure. *Geophysical Research Letters*, *33*, L04104. https://doi.org/10.1029/2005GL024969

Ebert, U., Nijdam, S., Li, C., Luque, A., Briels, T., & van Veldhuizen, E. (2010, 7). Review of recent results on streamer discharges and discussion of their relevance for sprites and lightning. *Journal of Geophysical Research*, *115*(A7), A00E43. https://doi.org/10.1029/2009ja014867

Gamerota, W. R., Cummer, S. A., Li, J., Stenbaek-Nielsen, H. C., Haaland, R. K., & McHarg, M. G. (2011). Comparison of sprite initiation altitudes between observations and models. *Journal of Geophysical Research*, *116*(2), A02317. https://doi.org/10.1029/2010JA016095

Gerken, E. A., & Inan, U. S. (2002). A survey of streamer and diffuse glow dynamics observed in sprites using telescopic imagery. *Journal of Geophysical Research*, *107*(A11), 1344. https://doi.org/10.1029/2002JA009248

Gordillo-Vázquez, F. J., & Luque, A. (2010, 8). Electrical conductivity in sprite streamer channels. *Geophysical Research Letters*, *37*(16), L16809. https://doi.org/10.1029/2010GL044349

Köhn, C., Chanrion, O., & Neubert, T. (2019). The sensitivity of sprite streamer inception on the initial electron-ion patch. *Journal of Geophysical Research: Space Physics*, *124*(4), 3083–3099. https://doi.org/10.1029/2018JA025972

Kulak, A., Kubisz, J., Klucjasz, S., Michalec, A., Mlynarczyk, J., Nieckarz, Z., et al. (2014). Extremely low frequency electromagnetic field measurements at the Hylaty station and methodology of signal analysis. *Radio Science*, *49*, 361–370. https://doi.org/10.1002/2014RS005400

Li, J., Cummer, S. A., Lyons, W. A., & Nelson, T. E. (2008). Coordinated analysis of delayed sprites with high-speed images and remote electromagnetic fields. *Journal of Geophysical Research Atmospheres*, *113*, D20206. https://doi.org/10.1029/2008JD010008

Luque, A., & Ebert, U. (2010). Sprites in varying air density: Charge conservation, glowing negative trails and changing velocity. *Geophysical Research Letters*, *37*(6), https://doi.org/10.1029/2009gl041982

Luque, A., Stenbaek-Nielsen, H. C., McHarg, M. G., & Haaland, R. K. (2016). Sprite beads and glows arising from the attachment instability in streamer channels. *Journal of Geophysical Research - A: Space Physics*, *121*, 2431–2449. https://doi.org/10.1002/2015JA022234

Malagón-Romero, A., Teunissen, J., Stenbaek-Nielsen, H. C., McHarg, M. G., Ebert, U., & Luque, A. (2020). On the emergence mechanism of carrot sprites. *Geophysical Research Letters*, *47*, e2019GL085776. https://doi.org/10.1029/2019GL085776

Mlynarczyk, J., Br, J., Kulak, A., Popek, M., & Kubisz, J. (2015). An unusual sequence of sprites followed by a secondary TLE: An analysis of ELF radio measurements and optical observations. *Journal of Geophysical Research: Space Physics*, *120*, 2241–2254. https://doi.org/10.1002/2014JA020780

Montanyà, J., Van Der Velde, O., Romero, D., March, V., Solà, G., Pineda, N., et al. (2010). High-speed intensified video recordings of sprites and elves over the western Mediterranean Sea during winter thunderstorms. *Journal of Geophysical Research*, *115*, A00E18. https://doi.org/10.1029/2009JA014508

Neubert, T., & Chanrion, O. (2013). On the electric breakdown field of the mesosphere and the influence of electron detachment. *Geophysical Research Letters*, *40*(10), 2373–2377. https://doi.org/10.1002/grl.50433

Pasko, V. P., Inan, U. S., & Bell, T. F. (2000). Fractal structure of sprites. *Geophysical Research Letters*, *27*(4), 497–500. https://doi.org/10.1029/1999GL010749

Pasko, V. P., Inan, U. S., Bell, T. F., & Taranenko, Y. N. (1997). Sprites produced by quasi-electrostatic heating and ionization in the lower ionosphere. *Journal of Geophysical Research*, *102*, 4529–4561. https://doi.org/10.1029/96JA03528

Pasko, V. P., Yair, Y., & Kuo, C. L. (2012). Lightning related transient luminous events at high altitude in the earth's atmosphere: Phenomenology, mechanisms and effects. *Space Science Reviews*, *168*(1–4), 475–516. https://doi.org/10.1007/s11214-011-9813-9

Qin, J., Pasko, V. P., McHarg, M. G., & Stenbaek-Nielsen, H. C. (2014). Plasma irregularities in the D-region ionosphere in association with sprite streamer initiation. *Nature Communications*, *5*(1), 3740. https://doi.org/10.1038/ncomms4740

Raizer, Y. P. (1997). *Gas discharge physics illustrated*. University of MichiganSpringer Berlin Heidelberg.

Savtchenko, A., Mitzeva, R., Tsenova, B., & Kolev, S. (2009). Analysis of lightning activity in two thunderstorm systems producing sprites in France. *Journal of Atmospheric and Solar-Terrestrial Physics*, *71*(12), 1277–1286. https://doi.org/10.1016/j.jastp.2009.04.010

Sentman, D. D., Wescott, E. M., Osborne, D. L., Hampton, D. L., & Heavner, M. J. (1995). Preliminary results from the Sprites94 aircraft campaign: 1. Red sprites. *Geophysical Research Letters*. *22*(10), 1205–1208. https://doi.org/10.1029/95GL00583

Soula, S., van der Velde, O., Montanyà, J., Neubert, T., Chanrion, O., & Ganot, M. (2009). Analysis of thunderstorm and lightning activity associated with sprites observed during the EuroSprite campaigns: Two case studies. *Atmospheric Research*, *9*(2–4), 514–528. https://doi.org/10.1016/j.atmosres.2008.06.017

Stenbaek-Nielsen, H. C., Kanmae, T., McHarg, M. G., & Haaland, R. (2013). High-speed observations of sprite streamers. *Surveys in Geophysics*, *34*, 769–795. https://doi.org/10.1007/s10712-013-9224-4

Stenbaek-Nielsen, H. C., & McHarg, M. G. (2008). High time-resolution sprite imaging: Observations and implications. *Journal of Physics D: Applied Physics*, *41*(23), 234009. https://doi.org/10.1088/0022-3727/41/23/234009

Suszcynsky, D. M., Strabley, R., Roussel-Dupre, R., Symbalisty, E. M., Armstrong, R. A., Lyons, W. A., & Taylor, M. (1999). Video and photometric observations of a sprite in coincidence with a meteor-triggered jet event. *Journal of Geophysical Research Atmospheres*, *104*(D24), 31361–31367. https://doi.org/10.1029/1999JD900962

van der Velde, O. A., Mika, A., Soula, S., Haldoupis, C., Neubert, T., & Inan, U. S. (2006). Observations of the relationship between sprite morphology and in-cloud lightning processes. *Journal of Geophysical Research Atmospheres*, *111*, D15203. https://doi.org/10.1029/2005JD006879

Williams, E., Downes, E., Boldi, R., Lyons, W., & Heckman, S. (2007). Polarity asymmetry of sprite-producing lightning: A paradox? *Radio Science*, *42*, RS2S17. https://doi.org/10.1029/2006RS003488